Nanoscale

Accepted Manuscript

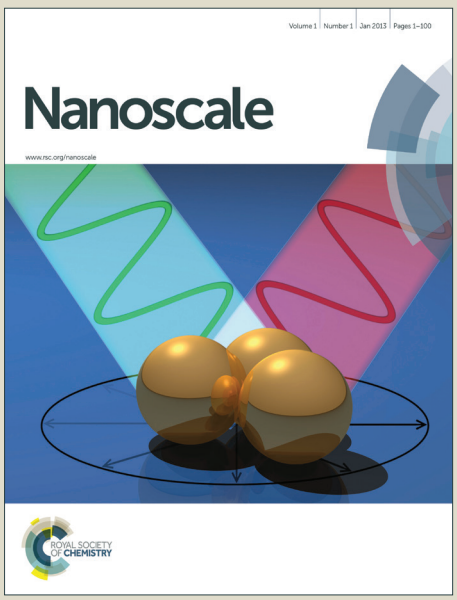

ROYAL SOCIETY OF CHEMISTRY

www.rsc.org/nanoscale

A Scanning Tunneling Microscope Break Junction Method with Continuous Bias Modulation

Edward Beall, Xing Yin, David H. Waldeck,* Emil Wierzbinski*

Department of Chemistry, University of Pittsburgh, Pittsburgh, PA 15260

Corresponding authors: dave@pitt.edu, emw40@pitt.edu

Abstract

Single molecule conductance measurements on 1,8-octanedithiol were performed using the Scanning Tunneling Microscope Break Junction method with an externally controlled modulation of the bias voltage. Application of an AC voltage is shown to improve the signal to noise ratio of low current (low conductance) measurements as compared to the DC bias method. The experimental results show that the current response of the molecule(s) trapped in the junction and the solvent media to the bias modulation can be qualitatively different. A model RC circuit which accommodates both the molecule and the solvent is proposed to analyze the data and extract a conductance for the molecule.

Keywords: single molecule, conductance, solvent capacitance, AC bias, RC circuit

Introduction

Development of experimental methods for determining the charge transfer properties of organic molecules has evolved to allow measurements on individual molecules.[1-4] Among the measurement methods the scanning tunneling microscope break junction (STM-BJ) has earned considerable popularity because of its simplicity and high measurement rate and because of the ability to make measurements on a variety of molecules and their conformers.[1] In STM-BJ the STM tip is repeatedly brought into contact with the substrate and then pulled away (withdrawn). This process forms a tip-substrate gap that is narrow enough to be bridged by a molecule(s) of sub-nanometer to nanometer length range. At a constant applied bias, the presence of a molecule(s) in the break junction gives rise to a non-zero current that is manifested as a plateau or series of plateaus in the current versus tip displacement curves. The magnitude of the current in the plateau is related to the conductance of the molecules and their number in the junction.

Several improvements to the method have expanded its applicability and the amount of the information provided by each experiment. One set of modifications focuses on mechanical modulation of the STM-BJ.[5-7] Control over the tip – substrate separation in these experimental approaches is accomplished by modulation of the extension/contraction of the piezoelement controlling the z-direction movement of the STM tip. Therefore, a transition between different molecular conformations can be probed with greater control than in the traditional STM-BJ,

which uses a constant tip withdrawal rate.[5, 7] Furthermore, the application of a continuous, high frequency, low amplitude modulation in the piezoelement movement provides help in resolving changes in the arrangement of the molecule-electrode contact or molecule conformation in the junction; in particular in differentiating a junction occupied by a molecule from an empty gap between the junction electrodes.[6] In a related set of STM-BJ modifications, modulation of the bias voltage within the STM-BJ is accomplished, and it is performed by sweeping the bias voltage while the position of the STM tip is stopped during the withdrawal in STM-BJ.[8-10] Recently, Adak et al. applied a small amplitude, 22 kHz AC sinusoidal modulation in addition to a constant DC bias rather than linear bias sweeps, in order to determine details of energy alignment and electronic couplings between molecular levels of pyridine-linked molecular bridges and gold and silver electrodes.[11] Application of such procedures can provide more information about the molecular junction than that in a constant bias junction. These methods require rigorous control of the STM tip movement and extreme tip position stability, however.

This work describes a simple experimental procedure, in which single molecule current-voltage curves are collected for the STM BJ under a constant tip movement. In this procedure we utilize the same tip crashing-withdrawal procedure as typically used in STM-BJ, but instead of applying a constant bias from the STM controller, a modulation voltage is applied continuously from an external voltage source. The present work focuses on a symmetrical triangular bias waveform (linear voltage-time sweeps in every modulation period with the same sweep rate in up and down directions) between 0 and 0.6 V.[12, 13] Current responses are collected for a voltage bias modulation over the frequency range of 500 – 2000 Hz. The workable range of applied modulation frequency is limited by the duration of the junction and sampling time, on the low and high frequency end, respectively.

Results and Discussion

A schematic illustration of a junction with the gold tip withdrawn at a constant rate from the gold substrate, in the presence of 1,8-octanedithiol in an organic solvent is shown in Figure 1A. In the experiment, the electrical current flowing through the junction is measured as a function of voltage and tip displacement (or time). The current traces consist of three main characteristic regions: (i) a rapid exponential current drop after the break of the metal-metal nanowire contact between the electrodes; (ii) an intermediate state in which current flows through the molecules spanning the electrodes (indicated by arrows in Figure 1B,C), and (iii) a low current condition at large tip-surface separations. In the case of a modulated bias, the magnitude of the current varies with the potential bias applied at any given moment; thus the measured current varies with the frequency of the bias voltage waveform. The current traces obtained in the absence of a molecule(s) in the junction are also different under constant and modulated bias conditions. While under constant bias the current remains constant (nominally zero) after the initial exponential drop; it oscillates around zero when a bias modulation is applied.

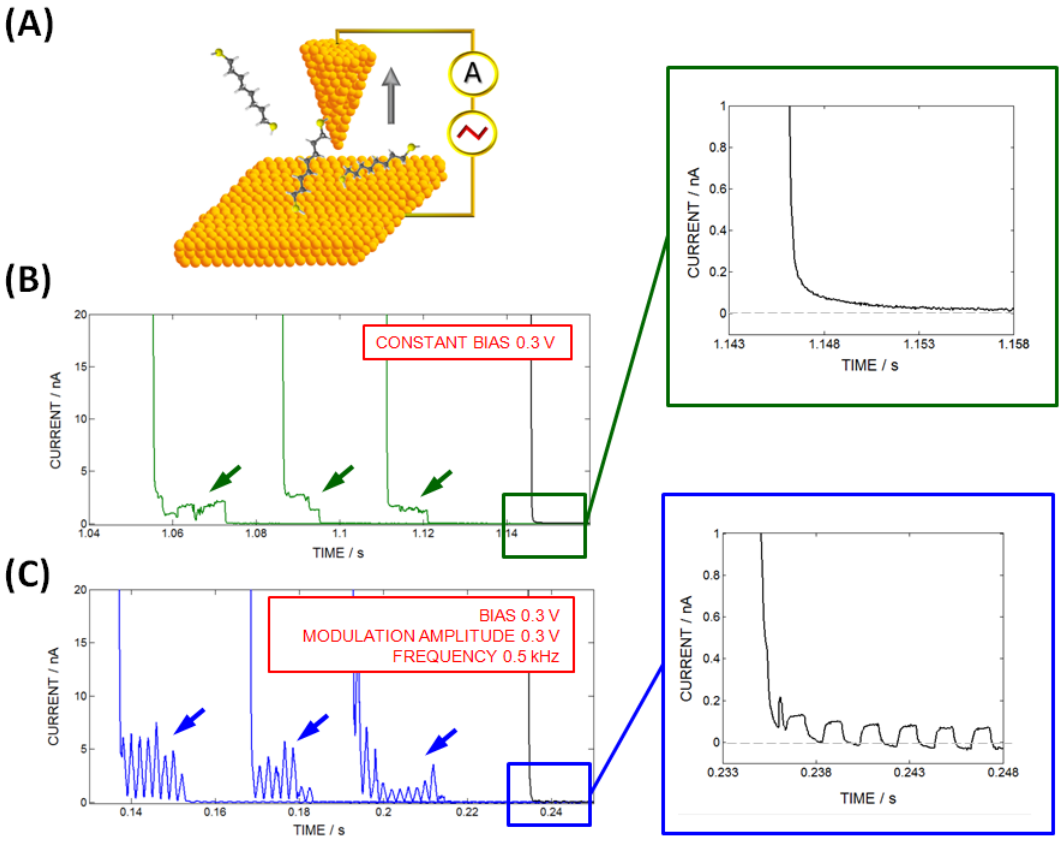

Figure 1. Panel A shows a schematic illustration of the molecular junction formed in a scanning tunneling microscope with a gold tip and gold substrates as the electrodes. Panels B and C show sample current – time traces obtained in the presence of 1,8-octanedithiol in mesitylene solvent, measured under a constant bias of 0.3 V (B) and a modulated bias of 0.3 ± 0.3 V (C). In both cases the retraction speed is 40 nm/s. Black traces in B and C are characteristic for molecule-free junctions. Arrows indicate the current responses of the molecules trapped in the junction.

In the absence of any molecule(s) bound in the junction (i.e., solvent only), the measurement displays a charging current waveform. This waveform originates from the STM tip and the substrate electrode serving as a capacitor. The capacitance is characteristic for a given experimental system and depends on the surface area of the substrate electrode, diameter of the wire used for preparation of the STM tip, and the volume of the solvent in the experimental liquid cell. These geometrical parameters were kept constant in our measurements, and a consistent current response was observed over a few months time. A uniform amplitude response was recorded for the STM tip –substrate separations between a few angstroms to 40 nm (the amplitude of the charging current waveform is very weakly dependent on the STM tip – substrate separation: about one percent decrease per 100 micrometers). Detailed information on the dependence of the geometrical factors on the response of the junction to the bias voltage is provided in the Supporting Material. The capacitance response displays strong sensitivity to the

solvent used in the measurements (see Figure 2). Figure 2 A-C shows current waveforms measured for mesitylene, 2,4-dichlorotoluene, and 3,4-dichlorotoluene, and can be rationalized by a simple RC circuit model. The amplitude of the current modulation increases with the polarity of solvent. Note the change in current scale for panels A, B, and C. Because of the different solvent molecule polarities, their dielectric constants are different, which leads to a change in the junction's capacitance. For mesitylene, the current waveform resembles closely the square wave characteristic that is expected for an in-series capacitor-resistor circuit below its frequency cutoff (i.e., the duration of the voltage modulation period is longer than the time constant of the circuit, see Supporting Materials). For the dichlorotoluene solvents, the junction response has a longer time constant and the current waveform becomes more triangular; i.e., is passed by the junction with less attenuation and less distortion (see Supporting Material for more detail). Figure 2D shows the calculated dipole moment of the solvent molecules under an increasing electrical field. Note that the static dipole moment of the solvent molecules increases from mesitylene (0 D) to 3,4-dichlorotoluene (3.1 D) and the induced dipole moment increases linearly with the strength of the applied electric field. The deformation of the current waveform decreases for mesitylene at higher frequency of the bias modulation (see Supporting Material). A more detailed description of the model equivalent circuit developed for the solvent is provided later in the text. The data in Figure 2 reveal that the solvent affects the current response to a voltage sweep in the molecular junction, and it must be considered when quantifying the overall current signal through the molecular junction.

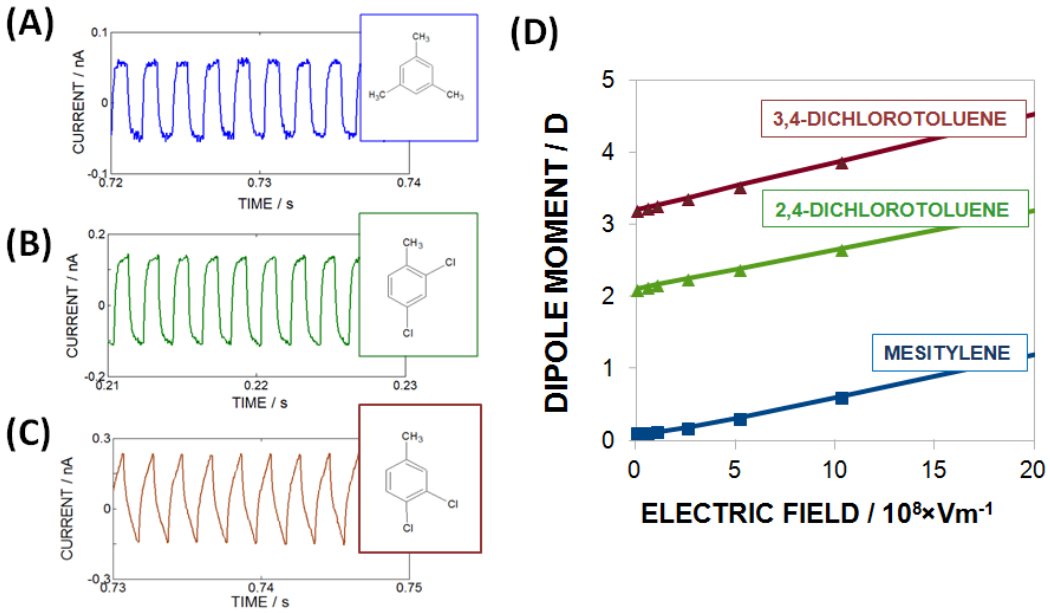

Figure 2. Panels A through C show current responses of the solvent under a bias voltage of 0.3 V that is modulated by 0.3 V at a frequency of 500 Hz for (A) mesitylene (dielectric constant ε=2.28) [14], (B) 2,4-dichlorotoluene (ε=5.68)[14], and (C) 3,4-dichlorotoluene (ε=8.97)[15]. Panel D shows calculated results for the influence of the electrical field strength on the dipole moment induced in these molecules. Note that zero electric field corresponds to the static dipole moment of the solvent molecules.

If octanedithiol molecules are present, the amplitude of the bias induced current oscillations through the junction is significantly higher than that of the mesitylene solvent (Figure 3A) or the 2,4-dichlorotoluene solvent (Figure 3B). Furthermore, the current waveforms become triangular and are offset from the zero current. This behavior is consistent with a resistance in parallel with the junction capacitance. If ohmic behavior is assumed for the molecule in the junction, the variations in the current amplitude within the experimental trace can be explained by the changes in the resistance from the molecule(s) in the junction during the course of the junction extension. Note that the presence of the adlayer of the octanedithiol molecules on the gold substrate surface does not have a noticeable influence on the solvent capacitive charging current waveform.

In the STM-BJ method, a large number of individual molecules and their conformations can be probed by repeating the experiment many times. This process allows one to construct distributions of the observed current. Because these global distributions are constructed by summation of the distributions built from many individual traces, they represent a property of the ensemble rather than the behavior of a given molecule. For the case of measurements under constant bias, the currents within the plateaus observed on the individual traces are observed more often than other fragments of the trace, so that peaks are formed in the current distributions. For the modulated bias case, the measured current varies with applied bias and the current response is sampled over a voltage range, albeit narrow. The current distributions constructed from the data recorded under constant and modulated bias for 1,8-octanedithiol in mesitylene and 2,4-dichlorotoluene are shown in Figure 3C. All the distributions show a main peak around 1 nA, and an additional small shoulder from 0.05 to 0.15 nA. The position of the ~ 1 nA peak is independent of the measurement method (DC versus modulated bias), which indicates that the solvent's response to the applied bias modulation has a negligible effect on the measured current, when it produces a current response that is higher than the solvent alone. For low currents measured in the junction (< 0.5 nA) the peak is shifted towards higher values when the bias modulation method is used. The magnitude of that shift is proportional to the current response of the solvent and it is notably bigger in 2,4-dichlorotoluene than in mesitylene.

We note that the solvent conditions may influence the conductance of the molecular bridge by causing the shift in the alignment of its molecular levels with respect to the Fermi levels of the electrodes and broadening of the bridge energy level distribution, as it has been shown by theoretical predictions.[16] Previous experimental studies show no[17] or only a week effect[18] of the solvent on the molecular conductance, however. In the present studies, a similar position of the current peak at ~ 1 nA in the current distributions of 1,8-octanedithiol in 2,4-dichlorotoluene and in 3,4-dichlorotoluene (see Figure 3C) indicates that the solvent does not affect the molecular conductance of the dithiol significantly, but contributes in parallel to the current measured in the junction.

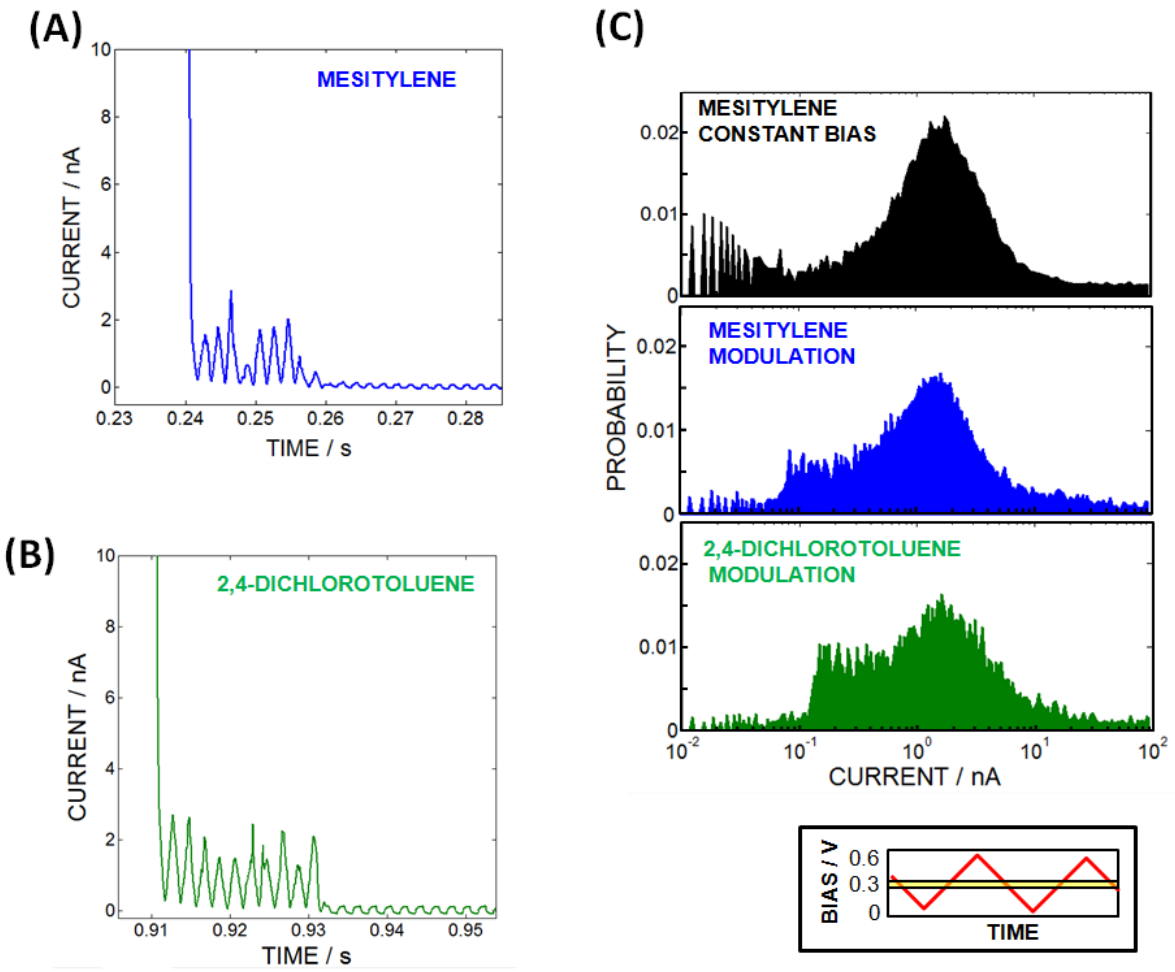

Figure 3. Panels A and B show sample current – time traces obtained in the presence of 1,8-octanedithiol in mesitylene (A) and in 2,4-dichlorotoluene (B) solvent, measured under a bias of 0.3 ± 0.3 V modulated with frequency of 500 Hz. Panel C shows histograms of many current versus time traces, measured in mesitylene and in 2,4-dichlorotoluene. The currents corresponding to a narrow 0.29 – 0.31 V range of applied bias (shown schematically in the inset in panel C as yellow box) were extracted to construct the distributions. Data obtained under constant bias of 0.3 V in mesitylene is shown for comparison. The current response characteristic for the solvent was not included in the analysis.

To quantify the influence of the solvent and to extract the conductance of the molecule from the current measured in the octanedithiol junction, simulations of the current response arising from the applied bias were performed with a model electrical circuit, using Matlab Simulink software. Figure 4A shows a comparison of an experimental current – time trace (black diamonds) with that simulated by an RC circuit (red curve). In this model the octanedithiol molecule is treated as a resistor that acts in parallel to the solvent, which is modeled as a resistor and capacitor in series. Parameters of the solvent RC circuit (yellow rectangular in Figure 4) were simulated first to match the current response of the junction with only solvent (modulation periods number 9 and 10). Note that leakage current through the solvent (i.e., leaky capacitor

model) can be accounted for by including a resistor R_S'; however its effect is found to be negligible for mesitylene.

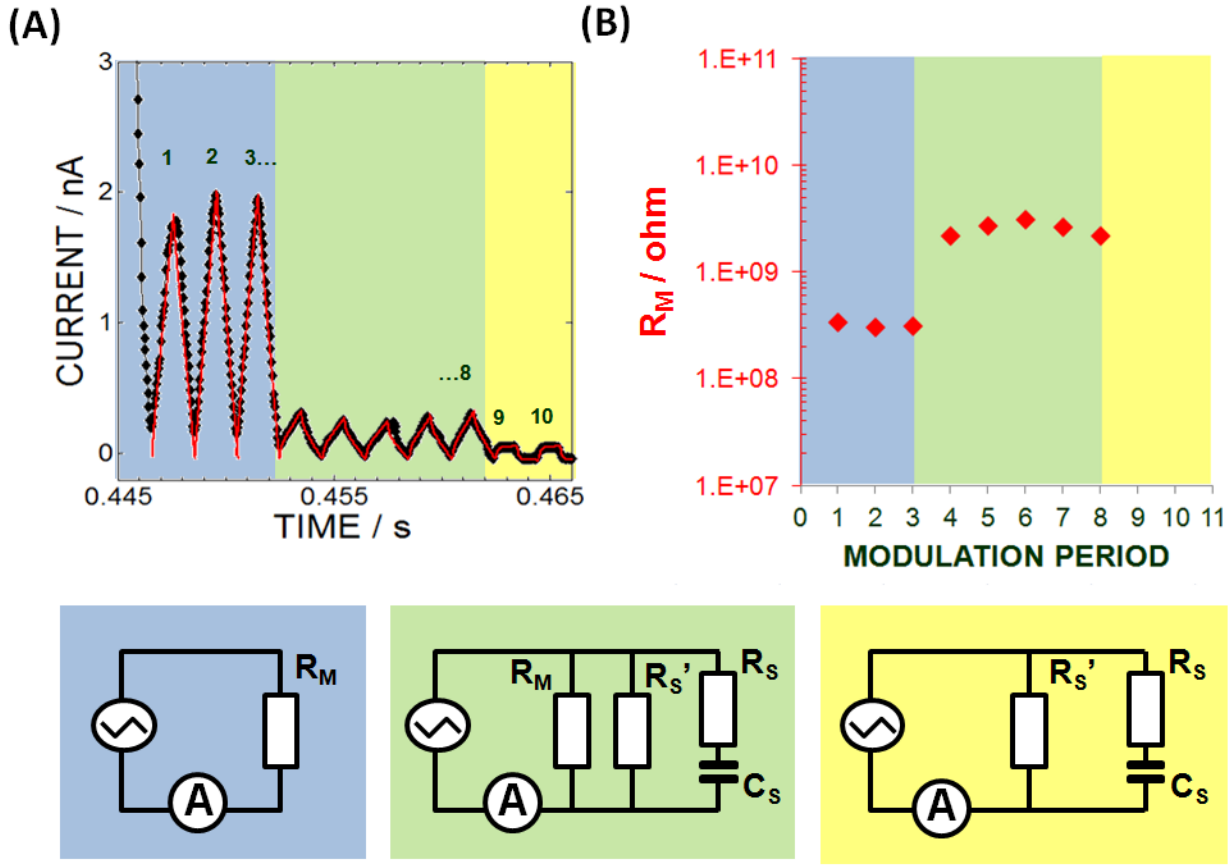

Figure 4. Results of fitting an experimental current versus time trace by a model electrical circuit. Panel A shows a sample experimental curve obtained in mesitylene under 0.3 ± 0.3 V bias modulation applied with 500 Hz frequency (black symbols), together with a simulated current response of the model electrical circuit (red lines). In the model electrical circuit, the measured molecule (1,8-octanedithiol) is represented as a resistor (R_M), and the solvent is modeled as a leaky capacitor [two resistors (R_S, R_S') and a capacitor (C_S)]. Parameters of the circuit elements associated with the solvent were kept constant (R_S'=1×10^{11} Ω, R_S=9×10^8 Ω, C_S=8.25×10^{-14} F). The simulations were performed to match each individual modulation period in the experimental curve using the most general circuit presented in the bottom row of the figure (green rectangle). Circuits in the blue and yellow rectangular region represent limiting approximations of the most general model circuit (green), in which the current response is determined solely by the molecule trapped in the junction (blue) or by the response of the solvent media alone (yellow). Panel B shows R_M values obtained for the 1,8-octanedithiol molecule in the current-time profile shown in panel A.

When an octanedithiol molecule is present in the junction, the amplitude of the current oscillations are higher than in the case of solvent alone. This change is modeled by a shunt resistance (R_M) that is associated with a molecule binding across the gap. Two distinct regions with two different resistances were present for the current trace of Figure 4A. In the region

highlighted with a green background, the amplitude of the current oscillations is closer to that observed for the solvent (mesitylene) alone than it is for the oscillations highlighted in blue. Furthermore, the current response shown in the green region has a shape that is intermediate between triangular (purely resistive) and square wave (purely capacitive). This distorted waveform reflects the combination of the solvent and the molecule on the response. In the region highlighted in blue, the current displays a triangular waveform with significantly higher amplitude than the solvent. In this current range, elimination of the solvent RC arm in the model electrical circuit causes little to no effect on the simulated current. Therefore, the equivalent circuit for this part of the trace can be simplified to the circuit shown in blue. Note that the distribution of the currents constructed for 1,8-octanedithiol in mesitylene from the modulated-bias data shown in Figure 3C is dominated by the peak with a maximum at 1-2 nA. In this regime the solvent response to the bias modulation is negligible and the current measured around 0.3 V bias was the same as in the case of the constant bias measurement.

The resistance of the molecule in the green and blue regions differs by nearly one order of magnitude, whereas within the blue or green region the resistances for the different cycles are within 30 % of each other. This observation is consistent with the presence of two different molecule-electrode conformations (low versus medium conductance) rather than a difference in the number of molecules effectively wired in the junction.[19-22] Within the blue region the fit gives a resistance of 0.32 ± 0.02 GΩ for the three cycles, and within the green region the fit gives a resistance of 2.55 ± 0.37 GΩ.

Figure 5 shows an example of an experimental trace, in which current oscillations are more complex. The trace is divided in a similar way to that in Figure 4, although notable current fluctuations are observed within the regions associated with octanedithiol. These variations between different modulation periods result in a change of simulated resistance close to a factor of two; thus it is very likely that the trace represents the situation in which two octanedithiol molecules are trapped simultaneously. Note that the bias voltage frequency applied in the experiment is relatively slow in comparison to the time for a molecule to 'jump' from one configuration to another in the junction; however its residence time in a particular geometry appears to last for many periods. Figure 5B shows examples of the modulation periods for which two simulations were performed to match different fragments of the data. Interestingly, the obtained R_M values correspond to the same resistances found for the other modulation periods, which is in agreement with the assumption of two molecules trapped in the junction (one or two equivalent resistors in parallel wired into the circuit); and they 'jump' between being 'wired' and not 'wired'.

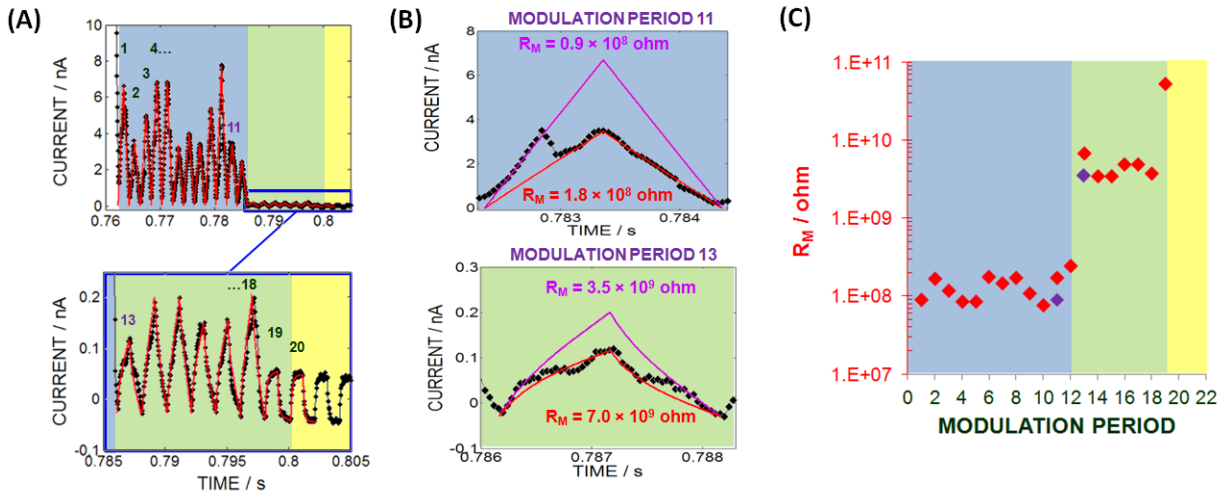

Figure 5. Results of fittings to experimental data with the model electrical circuit. Panel A shows a sample experimental curve obtained in mesitylene under 0.3 ± 0.3 V bias modulation applied with 500 Hz frequency (black symbols), together with a simulated current response of the model electrical circuit (red lines). Panel B shows examples of modulation periods, within which a change in the conformation of the molecules in the junction was observed. Only fits shown in red are included in panel A. Circuit parameters associated with the solvent are the same for all the simulated data (R_S'=1.0×10^{11} Ω, R_S=9.0×10^8 Ω, C_S=7.8×10^{-14} F). Panel C shows the fitted R_M value corresponding to subsequent modulation periods shown in panels A (red symbols) and B (violet symbols).

One would expect that a decrease of the modulation frequency would result in a larger number of the periods in which changes of the conformation of the molecule(s) in the junction are captured, and the information about the molecule(s)' conductance would more closely approximate the average of that for one and two molecules. The average resistance determined from all the periods within the blue region in Figure 4A is 0.13 ± 0.05 GΩ; however the current-time trace indicates a bimodal distribution of currents. The junction changes dynamically between two resistances, approximately 0.17 ± 0.03 GΩ and 0.09 ± 0.01 GΩ; see Figure 5C. Similarly, in the green region, the average resistance from all the periods gives 4.50 ± 1.30 GΩ, while distinct periods indicate two groups of resistances of 3.58 ± 1.26 GΩ and 5.68 ± 1.12 GΩ. In this study, the octanedithiol current-time traces were recorded at sub- kHz frequency of the bias voltage modulation, and the examples shown demonstrate that the kinetics of the molecule(s) binding in the junction can be probed at the single molecule level; i.e. within a single experimental trace. Application of even higher voltage modulation frequencies will likely prove to be even more beneficial for this type of quantification.

By collecting together data from one to two thousand curves, current-voltage distributions that correspond to an average electrical response of the ensemble of molecules can be constructed. Figure 6A shows an example of such a distribution for 1,8-octanedithiol. Importantly, it contains data at significantly more bias potentials than the characteristics constructed in traditional STM-

BJ (typically from less than ten bias voltages). For example, construction of such a two-dimensional distribution using constant bias would require one hundred and twenty datasets (typically a few hundred traces each) recorded between 0 and 0.6 V with 5 mV increments. In contrast to the measurements with the bias sweeps at constant tip position, the histogram obtained using the procedure presented in this manuscript gives averaged information over the ensemble of the molecules and conformations. Furthermore, because each experimental trace contains information about the response of the solvent, that information can be used to extract the resistance data of the molecule more reliably, in particular for small currents (low conductance).

Figure 6B shows the distribution of conductance values obtained for the same dataset as the current distributions shown in Figure 3C for mesitylene. The conductance values were obtained by matching the periods in the current-time traces to a library of current responses simulated using predefined R_M values. The main peak in the distribution, around 7×10^{-5} G_0, is close to the conductance reported for 1,8-octanedithiol (6×10^{-5} G_0),[19-21] while the broad peak/shoulder agrees with the reported value of ~1×10^{-6} G_0.[22] In all these literature studies, differences in the measured conductance were interpreted as originating from details of the Au-S contact. The distribution obtained using the modulated STM-BJ (blue histogram) and the DC bias method (black solid line) match with respect to the position of the conductance peaks. Nevertheless, in the case of modulated STM-BJ, the octanedithiol conductance is determined well over the entire available conductance range (with the lowest conductance restricted by the conductance of the pure solvent, and the high limit given by the sensitivity of STM preamplifier). In the case of DC measurements, the low conductance data (nominally calculated from the currents lower than 50 pA) is strongly affected by the sensitivity of the STM pre-amplifier and is very noisy.

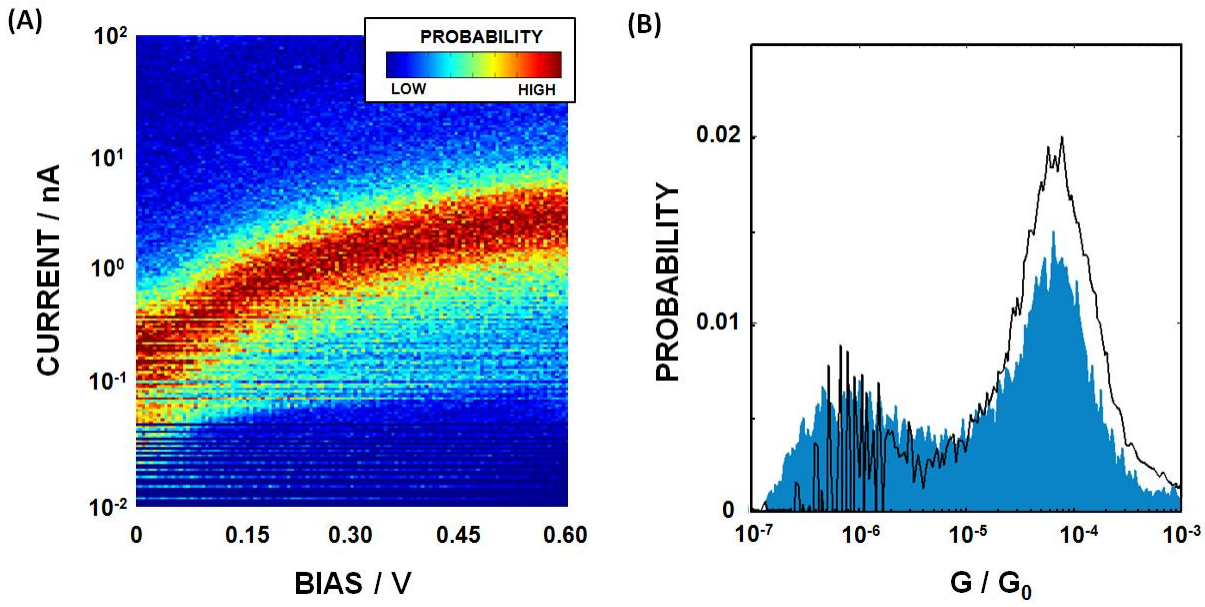

Figure 6. Panel A shows a two-dimensional current – voltage distribution constructed from two thousand current - time traces recorded for 1,8-octanedithiol in mesitylene under the bias modulation conditions of 0.3 ± 0.3 V (500 Hz). Because the bias voltage is generated continuously and is independent of the STM tip withdrawal procedure, the applied bias and the current measured in the junction were matched in phase based on the characteristic response of the solvent to the applied bias. Panel B shows the octanedithiol conductance distribution obtained by matching the modulation periods in experimental traces (blue histogram) with the library of two hundred current responses simulated for the circuits with predefined R_M values in a range 10^7-10^{11} ohm. Parameters of the circuit elements associated with the solvent were kept constant (R_S'=1×10^{11} Ω, R_S=9×10^8 Ω, C_S=8.25×10^{-14} F). The data is compared with the conductance distribution obtained using the constant bias STM BJ method (black curve). The conductance values are expressed in the units of the quantum conductance, $G_0 = 2e^2/h \approx 77$ μS.

Conclusions

In summary, a simple experimental procedure that allows current – voltage characterization of molecular junctions with high statistics was presented. The method is intermediate between the traditional STM BJ (with constant bias applied) and the procedures in which STM movement is controlled within the STM tip withdrawal in order to perform a bias voltage sweep, e.g. transition voltage spectroscopy. Importantly, the AC modulation method reveals the effect of the solvent medium on the response and allows it to be separated from that of the molecule bound across the junction. A model RC-circuit was shown to be useful for quantifying the effect of the solvent and the molecule in the junction. Application of the voltage modulation in molecular conductance measurements improves the extraction of low conductance data when compared to the constant voltage methodology. This study is a stepping stone towards the use of AC impedance methods for characterizing molecular tunnel junctions.

Methods

Conductance Measurements. The modulated-bias conductance measurements were performed using a variation on the STM-controlled break-junction method.[1] Through repeated cycles of precise retraction following a crashing of the STM tip, the studied molecule was able to occasionally form a molecular junction between the tip and substrate during the retraction period. The constant retraction speed of 40 nm/s was used in all measurements. During this process, an externally-generated modulated bias voltage (DS345 Function Generator, Stanford Research Systems) was applied in the form of a triangle wave to the bias voltage input of the STM breakout box. The tunneling current was subsequently monitored as a function of time; i.e. voltage and the tip-substrate distance. Piezoelement movement, current measurements, and the constant bias voltage (exclusively in control experiments) are regulated/measured by the STM which is controlled by standard software provided by the microscope vendor. In all measurements an STM scanner with a 10 nA/V pre-amplifier was used. Conductance values were determined through analysis of the current-distance plots as well as current-voltage characteristics (*vide infra*). All measurements were performed using an Agilent 5500 system with an environmental chamber housed in a homemade acoustically isolated Faraday cage. The cage sits on an active Table Stable anti-vibration system mounted on an optical table.

Sample Preparation. Ultraflat template-stripped gold substrates[23] were used. For substrate preparation, a 100 nm gold film was evaporated using a Thermionics VE-180 E-beam evaporator on freshly cleaved mica. Glass slips (10 mm x 25 mm) were affixed to the bare gold and the film was transferred to a glass slip prior to each experiment. The newly exposed atomically flat gold substrates were immersed for 20-30 seconds in a 2 mM 1,8-octanedithiol solution in ethanol, rinsed with ethanol and dried under an argon stream.

Data Collection. Experiments were performed using freshly cut gold STM tips (0.25 mm, 99.95% gold wire, Alfa Aesar). All experiments were performed under an argon atmosphere with the substrates in mesitlyene, 2,4-dichlorotoluene, or 3,4-dichlorotoluene. The modulation amplitude of the applied bias was ± 0.3 V with the triangle wave centered about 0.3 V and modulation frequencies ranging from 0.5 kHz to 2 kHz. Measurements were collected using a 10 nA/V preamplifier. Thousands of current-distance profiles were collected for each set of parameters, typically requiring several independent substrates and multiple STM tips to be used in order to amass sufficient data.

Data Analysis. Home-written Matlab scripts were used for current-distance plot data filtering and analysis. Plots displaying current plateaus were selected from the set of thousands of traces and the current response was matched to the generated triangle-wave bias in order to determine the respective applied bias for every current data point.

A three-dimensional distribution was generated with a logarithmically scaled current axis having 25 bins per decade and a linearly scaled applied bias axis having 25 bins per 0.1 V. The color-scaled surface can then be partitioned to show a normalized histogram for a specific bias.

The conductance values were obtained by matching individual periods in the current – time traces with the library of two hundred current responses simulated using model circuit (green rectangular in Figure 4 in manuscript) with predefined R_M values spaced logarithmically between $10^7$and 10^{11} ohm. The quality of the match between experimental and simulated data was found by calculating the χ^2 defined as:

$$\chi^2 = \sum_n \left(\frac{i_{exp}(n) - i_{sym}(n)}{error(n)}\right)^2 \qquad \text{(Eqn. 1)}$$

where i_{exp} and i_{sym} are experimental and simulated current values for each data point '*n*' in a given period. A constant error of 5 pA was used for the currents below 100 pA, and 5 percent of the simulated current value for the remaining data points. The R_M value, for which the simulated response produced the smallest χ^2 was used. 10 percent of the periods with the highest χ^2 values out of the entire dataset were omitted in construction of the conductance distribution.

Calculation of the Dipole Moment of Solvent Molecules under Various Electrical Fields. Ground state geometry optimization was performed at the B3LYP/6-31G(d) level for mesitylene, 2,4-dichlorotuluene, and 3,4-dichlorotuluene using Gaussian 09.[24] An external electric field was applied along the direction of the intrinsic dipole moments during optimization. Although DFT methods are known to ignore dispersion, the hybrid B3LYP functional[25, 26] was found to be acceptable for comparing the trend among small organic molecules[27, 28] and thus was used in the calculations.

Acknowledgments

D.H.W. acknowledges support from NSF (DMR-1412030). Computational resources were provided by the Center for Simulation and Modeling (SaM) at the University of Pittsburgh.

Supporting Material

Electronic Supplementary Information (ESI) available: additional current – time traces recorded for mesitylene, 2,4-dichlorotoluene, and 3,4-dichlorotoluene under different bias modulation frequencies, determined solvent capacitance values, and traces recorded under various geometrical constraints in the experimental cell are provided.

References

1. B. Xu and N. J. Tao, *Science*, 2003, **301**, 1221.
2. X. D. Cui, A. Primak, X. Zarate, J. Tomfohr, O. F. Sankey, A. L. Moore, T. A. Moore, D. Gust, G. Harris and S. M. Lindsay, *Science*, 2001, **294**, 571.
3. M. A. Reed, C. Zhou, C. J. Muller, T. P. Burgin and J. M. Tour, *Science*, 1997, **278**, 252.
4. X. Guo, J. P. Small, J. E. Klare, Y. Wang, M. S. Purewal, I. W. Tam, B. H. Hong, R. Caldwell, L. Huang, S. O'Brien, J. Yan, R. Breslow, S. J. Wind, J. Hone, P. Kim and C. Nuckolls, *Science*, 2006, **311**, 356.
5. J. S. Meisner, M. Kamenetska, M. Krikorian, M. L. Steigerwald, L. Venkataraman and C. Nuckolls, *Nano Lett.*, 2011, **11**, 1575.
6. J. L. Xia, I. Diez-Perez and N. J. Tao, *Nano Lett.*, 2008, **8**, 1960.
7. J. Zhou, G. Chen and B. Xu, *J. Phys. Chem. C*, 2010, **114**, 8587.
8. J. M. Artés, M. López-Martínez, A. Giraudet, I. Díez-Pérez, F. Sanz and P. Gorostiza, *J. Am. Chem. Soc.*, 2012, **134**, 20218.
9. S. Guo, J. Hihath, I. Díez-Pérez and N. Tao, *J. Am. Chem. Soc.*, 2011, **133**, 19189.
10. K. Wang, J. Hamill, J. Zhou, C. Guo and B. Xu, *Faraday Discuss.*, 2014, **174**, 91.
11. O. Adak, R. Korytár, A. Y. Joe, F. Evers and L. Venkataraman, *Nano Lett.*, 2015, **15**, 3716.
12. *We slightly extended the bias voltage range for which linear current response to applied voltage was reported for 1,8-octanedithiol. (Morita T., Lindsay M, J. Am. Chem. Soc. 2007, 129, 7262)*
13. T. Morita and S. Lindsay, *J. Am. Chem. Soc.*, 2007, **129**, 7262.
14. *CRC Handbook of Chemistry and Physics 84th Ed.*, CRC Press, Boca Raton, FL, 2003.
15. R. R. Dreisbach, in *Physical Properties of Chemical Compounds*, American Chemical Society, 1961, vol. 15, ch. 1, pp. 3-523.
16. I. Baldea, *Nanoscale*, 2013, **5**, 9222.
17. H. van Zalinge, D. J. Schiffrin, A. D. Bates, W. Haiss, J. Ulstrup and R. J. Nichols, *ChemPhysChem*, 2006, **7**, 94.
18. V. Fatemi, M. Kamenetska, J. B. Neaton and L. Venkataraman, *Nano Lett.*, 2011, **11**, 1988.
19. F. Chen, X. Li, J. Hihath, Z. Huang and N. Tao, *J. Am. Chem. Soc.*, 2006, **128**, 15874.
20. W. Haiss, S. Martín, E. Leary, H. v. Zalinge, S. J. Higgins, L. Bouffier and R. J. Nichols, *J. Phys. Chem. C*, 2009, **113**, 5823.
21. C. Li, I. Pobelov, T. Wandlowski, A. Bagrets, A. Arnold and F. Evers, *J. Am. Chem. Soc.*, 2008, **130**, 318.
22. E. Wierzbinski and K. Slowinski, *Langmuir*, 2006, **22**, 5205.
23. M. Hegner, P. Wagner and G. Semenza, *Surf. Sci.*, 1993, **291**, 39.
24. M. J. Frisch, G. W. Trucks, H. B. Schlegel, G. E. Scuseria, M. A. Robb, J. R. Cheeseman, G. Scalmani, V. Barone, B. Mennucci, G. A. Petersson, H. Nakatsuji, M. Caricato, X. Li, H. P. Hratchian, A. F. Izmaylov, J. Bloino, G. Zheng, J. L. Sonnenberg, M. Hada, M. Ehara, K. Toyota, R. Fukuda, J. Hasegawa, M. Ishida, T. Nakajima, Y. Honda, O. Kitao, H. Nakai, T. Vreven, J. A. Montgomery Jr., J. E. Peralta, F. Ogliaro, M. J. Bearpark, J. Heyd, E. N. Brothers, K. N. Kudin, V. N. Staroverov, R. Kobayashi, J. Normand, K. Raghavachari, A. P. Rendell, J. C. Burant, S. S. Iyengar, J. Tomasi, M. Cossi, N. Rega, N. J. Millam, M. Klene, J. E. Knox, J. B. Cross, V. Bakken, C. Adamo, J. Jaramillo, R. Gomperts, R. E. Stratmann, O. Yazyev, A. J. Austin, R. Cammi, C. Pomelli, J. W.

Ochterski, R. L. Martin, K. Morokuma, V. G. Zakrzewski, G. A. Voth, P. Salvador, J. J. Dannenberg, S. Dapprich, A. D. Daniels, Ö. Farkas, J. B. Foresman, J. V. Ortiz, J. Cioslowski and D. J. Fox, *Gaussian 09 Revision B.01*, 2010.
25. A. D. Becke, *J. Chem. Phys.*, 1993, **98**, 5648.
26. C. Lee, W. Yang and R. G. Parr, *Phys. Rev. B*, 1988, **37**, 785.
27. Y. Li, J. Zhao, X. Yin and G. Yin, *J. Phys. Chem. A*, 2006, **110**, 11130.
28. X. Quan, C. W. Marvin, L. Seebald and G. R. Hutchison, *J. Phys. Chem. C*, 2013, **117**, 16783.